J Physiol 593.6 (2015) pp 1479–1493

The Journal of Physiology

Decreased inward rectifying K^+ current and increased ryanodine receptor sensitivity synergistically contribute to sustained focal arrhythmia in the intact rabbit heart

Rachel C. Myles[1], Lianguo Wang[2], Donald M. Bers[2] and Crystal M. Ripplinger[2]

[1] *Institute of Cardiovascular and Medical Sciences, University of Glasgow, Glasgow, UK*
[2] *Department of Pharmacology, School of Medicine, University of California, Davis, CA, USA*

Key points

- Heart failure leads to dramatic electrophysiological remodelling as a result of numerous cellular and tissue-level changes. Important cellular changes include increased sensitivity of ryanodine receptors (RyRs) to Ca^{2+} release and down-regulation of the inward rectifying K^+ current (I_{K1}), both of which contribute to triggered action potentials in isolated cells.
- We studied the role of increased RyR sensitivity and decreased I_{K1} in contributing to focal arrhythmia in the intact non-failing rabbit heart using optical mapping and pharmacological manipulation of RyRs and I_{K1}.
- Neither increased RyR sensitivity or decreased I_{K1} alone led to significant increases in arrhythmia following local sympathetic stimulation; however, in combination, these two factors led to a significant increase in premature ventricular complexes and focal ventricular tachycardia.
- These results suggest synergism between increased RyR sensitivity and decreased I_{K1} in contributing to focal arrhythmia in the intact heart and may provide important insights into novel anti-arrhythmic treatments in heart failure.

Abstract Heart failure (HF) results in dramatic electrophysiological remodelling, including increased sensitivity of ryanodine receptors (RyRs) and decreased inward rectifying K^+ current (I_{K1}), which predisposes HF myocytes to delayed afterdepolarizations and triggered activity. Therefore, we sought to determine the role of increased RyR sensitivity and decreased I_{K1} in contributing to focal arrhythmia in the intact non-failing heart. Optical mapping of transmembrane potential and intracellular Ca^{2+} was performed in Langendorff-perfused rabbit hearts ($n = 15$). Local β-adrenergic receptor stimulation with noradrenaline (norepinephrine; NA, 50 μl, 250 μM) was applied to elicit focal activity (premature ventricular complexes (PVCs) or ventricular tachycardia (VT $\geq$ 3 beats)). NA was administered under control conditions (CTL) and following pretreatment with 50 μM $BaCl_2$ to reduce I_{K1}, or 200 μM caffeine (Caff) to sensitize RyRs, both alone and in combination. Local NA injection resulted in Ca^{2+}-driven PVCs arising from the injection site in all hearts studied. No increase in NA-mediated PVCs was observed following pretreatment with either $BaCl_2$ or Caff alone (CTL: 1.1 $\pm$ 0.7, $BaCl_2$: 1.0 $\pm$ 0.7, Caff: 1.3 $\pm$ 0.8 PVCs/injection, P not significant). However, pretreatment with the combination of $BaCl_2$ + Caff resulted in a significant increase in PVCs (2.3 $\pm$ 2.8 PVCs/injection, $P < 0.05$ *vs.* CTL, $BaCl_2$, Caff). Additionally, pretreatment with $BaCl_2$ + Caff led to sustained monomorphic VT arising from the NA application site in all hearts studied, which lasted up to 6 min following a single NA injection. VT was never observed under any other condition suggesting synergism between increased RyR sensitivity and decreased I_{K1} in contributing to focal activity.

DOI: 10.1113/jphysiol.2014.279638

These findings may have important implications for the understanding and prevention of focal arrhythmia in HF.

(Received 20 June 2014; accepted after revision 30 August 2014; first published online 5 September 2014)
Corresponding author C. M. Ripplinger: Department of Pharmacology, UC Davis School of Medicine, 2219A Tupper Hall, One Shields Ave, Davis, CA 95616, USA. Email: cripplinger@ucdavis.edu

Abbreviations AP, action potential; APD, action potential duration; β-AR, β-adrenergic receptor; BCL, basic cycle length; Caff, caffeine; CaT, intracellular calcium transient; CaTD, intracellular calcium transient duration; DAD, delayed afterdepolarization; ECG, electrocardiogram; HF, heart failure; I_{K1}, inward rectifying K^+ current; NA, noradrenaline (norepinephrine); NCX, Na^+/Ca^{2+} exchanger; NT, normal Tyrode solution; PVC, premature ventricular complex; RyR, ryanodine receptor; SERCA, sarcoplasmic reticulum Ca^{2+}-ATPase; SR, sarcoplasmic reticulum; τ, time constant of calcium transient decay; V_m, transmembrane potential; VOP, ventricular overdrive pacing; VT, ventricular tachycardia.

Introduction

Heart failure (HF) is a common condition associated with extremely high mortality (Baker *et al.* 2003; McMurray & Pfeffer, 2005). Approximately half of all HF deaths occur suddenly, primarily from ventricular tachycardia (VT) degenerating into ventricular fibrillation (Huikuri *et al.* 2001). Although re-entry may be responsible for initiation and maintenance of arrhythmia in many pathological states, there is compelling evidence that VT in non-ischaemic HF arises via focal (non-re-entrant) mechanisms (Vermeulen *et al.* 1994; Pogwizd, 1995; Pogwizd *et al.* 1998, 2001; Hoeker *et al.* 2009). Three-dimensional cardiac mapping in a rabbit model of pressure and volume overload HF has revealed that spontaneous VT is initiated and maintained by focal activity (Pogwizd, 1995). Similar mapping studies on explanted human hearts with non-ischaemic HF showed that both spontaneous and inducible VT occurred by focal mechanisms (Pogwizd *et al.* 1998). This focal activity is likely triggered by premature ventricular complexes (PVCs) that arise via early- or delayed afterdepolarizations (EADs, DADs).

At the cellular level, DADs occur after repolarization and are due to spontaneous sarcoplasmic reticulum (SR) Ca^{2+} release. This rise in intracellular Ca^{2+} ($[Ca^{2+}]_i$) leads to Ca^{2+} extrusion via the Na^+/Ca^{2+} exchanger (NCX). Because NCX is electrogenic, Ca^{2+} efflux produces a depolarizing inward current that, if of sufficient magnitude, will result in a DAD. At the tissue level, however, in order for a DAD to propagate as a PVC, a critical number of myocytes must all have DADs *simultaneously* in order to overcome the source–sink mismatch (Joyner & van Capelle, 1986; Xie *et al.* 2010). We recently showed localized β-adrenergic receptor (β-AR) stimulation as a mechanism of DADs and PVC initiation in the intact healthy rabbit heart via spatio-temporal synchronization of SR Ca^{2+} overload and release (Myles *et al.* 2012). We further showed that partial gap junction uncoupling increases the likelihood of inducing PVCs with local β-ARs by decreasing the source–sink mismatch. However, even with partial gap junction uncoupling, arrhythmias induced by local β-ARs were generally limited to isolated PVCs, couplets, or triplets and sustained VT was not observed, thus providing limited insight into the underlying mechanisms of sustained focal ventricular arrhythmia.

Several key characteristics have been identified that predispose HF myocytes to DADs and triggered action potentials (APs), including a down-regulation of the inward rectifying K^+ current, I_{K1} (Pogwizd *et al.* 2001), which normally stabilizes the resting membrane potential (V_m). Therefore, during spontaneous SR Ca^{2+} release, the depolarizing current carried by NCX causes larger amplitude DADs and increases the likelihood of reaching threshold for an AP (Puglisi & Bers, 2001). Furthermore, HF myocytes show increased SR Ca^{2+} leak via ryanodine receptors (RyRs) (Shannon *et al.* 2003) and preserved β-AR responsiveness (Pogwizd *et al.* 2001). Hence, the goal of the present study was to determine the individual and combined role of these key HF phenotypes (decreased I_{K1}, increased RyR sensitivity) in contributing to focal arrhythmia during local β-AR stimulation in the intact non-failing rabbit heart. Specifically, we reduced I_{K1} with $BaCl_2$ (50 μM) (Foster *et al.* 1977; Pogwizd *et al.* 2001) and increased the sensitivity of RyR with low-dose caffeine (200 μM) (Trafford *et al.* 1998; Wang *et al.* 2014). These interventions were investigated both alone and in combination to determine the resulting effects on focal arrhythmia susceptibility. Interestingly, at the doses studied, neither intervention alone increased the likelihood of PVCs or focal activity, but together they were strikingly pro-arrhythmic, often resulting in sustained focal ventricular arrhythmia. These findings suggest that significant synergism exists between these two key cellular phenotypes in contributing to focal arrhythmias in the intact heart and the results of this study may have important clinical implications for the understanding and prevention of focal arrhythmia in HF where these two phenotypes may co-exist.

Methods

Ethical approval

All procedures involving animals were approved by the Animal Care and Use Committee of the University of California, Davis, and adhered to the *Guide for the Care and Use of Laboratory Animals* published by the US National Institutes of Health (NIH Publication No. 85-23, revised 1996). The authors have read, and the experiments comply with, the policies and regulations of *The Journal of Physiology* given by Drummond (2009).

Langendorff-perfused rabbit hearts

Male New Zealand White rabbits ($n = 15$) weighing 3–4 kg were anaesthetized with a single intravenous injection of pentobarbital sodium (50 mg kg^{-1}) containing 1000 IU of heparin. Following a midsternal incision, hearts were rapidly excised and Langendorff-perfused at 37°C with oxygenated (95% O_2, 5% CO_2) modified Tyrode solution of the following composition (in mM): NaCl 128.2, $CaCl_2$ 1.3, KCl 4.7, $MgCl_2$ 1.05, NaH_2PO_4 1.19, $NaHCO_3$ 20 and glucose 11.1 (pH 7.4 ± 0.05). Flow rate (25–35 ml min^{-1}) was adjusted to maintain a perfusion pressure of 60–70 mmHg. One leaflet of the mitral valve was carefully damaged with sharp forceps inserted through the pulmonary vein to prevent solution congestion after the suppression of ventricular contraction. This also prevented acidification of the perfusate and the development of ischaemia in the left ventricle. Two Ag/AgCl disc electrodes were positioned in the bath to record an electrocardiogram (ECG) analogous to a lead I configuration. Bipolar pacing electrodes were positioned on the base of the left ventricular epicardium for pacing, which was performed at a basic cycle length (BCL) of 300 ms using a 2 ms pulse at twice the diastolic threshold.

Dual optical mapping of V_m and Ca^{2+}

Dual optical mapping was performed as previously described (Myles *et al.* 2012). Hearts were loaded with the acetoxymethyl ester form of the fluorescent intracellular Ca^{2+} indicator Rhod-2 (Rhod-2 AM; Molecular Probes, Eugene, OR, USA; 0.5 ml of 1 mg ml^{-1} in dimethyl sulfoxide (DMSO) containing 10% pluronic acid) and were subsequently stained with the voltage-sensitive dye RH237 (Molecular Probes; 50 μl of 1 mg ml^{-1} in DMSO). Blebbistatin (Tocris Bioscience, Ellisville, MO, USA; 10–20 μM) was added to the perfusate to eliminate motion artifact during optical recordings (Fedorov *et al.* 2007). The anterior epicardial surface including the right and left ventricles was excited using LED light sources centred at 530 nm and bandpass filtered from 511 to 551 nm (LEX-2, SciMedia, Costa Mesa, CA, USA) and focused directly on the surface of the preparation. The emitted fluorescence was collected through a 25 mm objective (Navitar, Japan) and split with a dichroic mirror at 630 nm. The longer wavelength moiety, containing the V_m signal, was longpass filtered at 700 nm and the shorter wavelength moiety, containing the Ca^{2+} signal, was bandpass filtered with a 32 nm filter centred at 590 nm. The emitted fluorescence signals were then recorded using two CMOS cameras (MiCam Ultima-L, SciMedia, Costa Mesa, CA, USA) with a sampling rate of 1 kHz and 100 pixels × 100 pixels with a 35 mm × 35 mm field of view.

Experimental protocol

Baseline electrophysiological parameters were determined during epicardial pacing at a BCL of 300 ms. The sino-atrial node was removed to produce a slow atrial or junctional intrinsic rhythm to facilitate the escape of focal activity between beats. Localized β-AR stimulation was performed during intrinsic rhythm with local administration of noradrenaline (NA) as previously described (Myles *et al.* 2012). Subepicardial injections of NA were delivered via 30 G needles with a 90° bend 1.5 mm from the tip to control the depth of injection. Needles were connected to a length of PE-10 tubing attached to a 0.5 ml syringe to prevent motion at the needle tip during injections. Injections of normal Tyrode solution (NT, 50 μl: control) and NA (250 μM, 50 μl) were delivered. Following each NA injection, the tissue bath was washed out and refilled with fresh NT to ensure that NA did not accumulate in the perfusate. Injections for all protocols were limited to 4 × 50 μl injections per site, which we have previously demonstrated does not produce tissue damage or ischaemia, or alter electrophysiological properties (Myles *et al.* 2012). We performed NT and NA injections at each site and rotated between multiple injection sites to allow a delay between injections at the same site. Pharmacological intervention was then performed with (1) 50 μM $BaCl_2$ to decrease I_{K1} ($n = 6$), (2) caffeine (Caff, 200 μM) to sensitize RyRs ($n = 5$), or (3) a combination of $BaCl_2$ and caffeine ($BaCl_2$ + Caff, $n = 6$). In each case the drug was allowed to equilibrate for a period of 10 min, during which time ventricular pacing at 300 ms was applied at regular intervals to allow for comparison of V_m and Ca^{2+} characteristics with baseline values, and to verify that steady state had been reached. The local injection protocol was then repeated during intrinsic rhythm. When assessing the impact of either drug, the same numbers of injections (both NT and NA) were tested at the same number of injection sites before and after drug. Coronary perfusion pressure was monitored throughout every experiment to ensure that there were no significant changes in perfusion pressure in response to any of the

pharmacological interventions, or to the injections of NA or NT.

Data analysis and statistics

Data analysis was performed using two different commercially available analysis programs (*BV_Analyze*, Brainvision, Tokyo, Japan; and *Optiq*, Cairn, UK). V_m and Ca^{2+} datasets were spatially aligned and processed with a Gaussian spatial filter (radius 3 pixels). For both APs and intracellular calcium transient (CaTs), activation time was determined as the time at 50% between peak and baseline amplitude and rise time as the time from 10 to 90% of the upstroke. For APs, repolarization time at 80% was determined at 80% of the return to baseline amplitude and action potential duration at 80% (APD_{80}) as repolarization time minus activation time. For CaTs, duration was measured at 50 and 80% ($CaTD_{50}$, $CaTD_{80}$, respectively) and the time course of decay was quantified using the time constant (τ) of a single exponential fit of the decay portion of the trace (from 30 to 100% of the downslope) (Laurita *et al.* 2003). For comparison of V_m and Ca^{2+} activation times, signals were normalized and activation maps were generated for each. V_m activation time was then subtracted from Ca^{2+} activation time for each pixel to produce maps of V_m–Ca^{2+} delay. Phase plots of the V_m/Ca^{2+} relationship at specific locations were generated by plotting the normalized V_m values (x-axis) against the normalized Ca^{2+} values (y-axis) for the time course of a single AP, where counter-clockwise chirality indicates normal V_m/Ca^{2+} coupling, and clockwise chirality indicates Ca^{2+} leading V_m (Choi *et al.* 2002). PVCs were identified by the presence of a broad QRS complex and a ventriculo-atrial activation sequence on the lead I ECG. For those PVCs that were optically mapped, activation maps were compared to those of intrinsic rhythm to verify a different origin and slower total activation time. VT was defined as ≥3 consecutive PVCs.

Continuous variables are presented as mean ± SD. Comparisons between two groups of continuous data were made using Student's t test, paired where appropriate, and categorical data using Fisher's exact test. Multiple comparisons were made using one- or two-way analysis of variance (ANOVA) with Bonferroni's post testing. $P < 0.05$ was considered statistically significant.

Results

Drug effects

Before assessing the contribution of each drug ($BaCl_2$, Caff, or $BaCl_2$ + Caff) to focal arrhythmia propensity, baseline electrophysiological parameters were compared before and after drug application with ventricular epicardial pacing at 300 ms. Example V_m and Ca^{2+} traces along with average APD_{80} and $CaTD_{80}$ before and after drug application are shown in Fig. 1. Caff alone had no significant effect on any parameter measured (AP rise time, CaT rise time, conduction velocity (data for these parameters not shown), or APD_{80}, $CaTD_{80}$). $BaCl_2$ alone significantly prolonged APD_{80} by approximately 10% (Fig. 1*B*, 173 *vs.* 190 ms, $P < 0.05$), consistent with prolongation of terminal repolarization due to decreased I_{K1}. All other parameters remained unchanged with $BaCl_2$. When $BaCl_2$ and Caff were combined, APD_{80} was prolonged to a degree similar to that with $BaCl_2$ alone; however, $CaTD_{80}$ was also slightly prolonged (approximately 5%, Fig. 1*D*). This prolongation of $CaTD_{80}$ does not appear to be associated with the addition of Caff, as Caff alone tended to shorten, not prolong $CaTD_{80}$, and may therefore be secondary to APD prolongation with $BaCl_2$.

Localized β-AR-induced PVCs

Consistent with previous studies (Myles *et al.* 2012), local application of NA under all conditions resulted in a greater incidence of PVCs compared to NT application (Table 1). Under all conditions, NA-induced PVCs were characterized by a broad QRS complex, ventriculo-atrial activation sequence on the ECG (Fig. 2*A*) and ventricular activation arising from the injection site on activation maps (Fig. 2*B*). Importantly, under all conditions, the V_m–Ca^{2+} delay revealed pathological early Ca^{2+} release at the site of initiation that likely drives membrane depolarization, consistent with β-AR-mediated SR Ca^{2+} overload and release (Fig. 2*B*) (Myles *et al.* 2012). Comparison of the superimposed APs and CaTs demonstrates the simultaneous upstrokes during NA-induced PVCs (Fig. 2*C*) which result in abnormal chirality of the V_m/Ca^{2+} phase plots (Fig. 2*D*). Surprisingly, neither $BaCl_2$ nor Caff alone had a significant impact on the propensity to local β-AR-induced PVCs (Table 1), suggesting that, in isolation, neither a destabilized resting V_m (as is the case with $BaCl_2$) or sensitized RyRs (with Caff) at the magnitudes tested in the current study are particularly arrhythmogenic. However, when the same doses of each drug were combined ($BaCl_2$ + Caff), a significant increase in NA-induced PVCs was observed (Table 1, Fig. 2*E*) without any increase in NT-induced PVCs.

Localized β-AR-induced focal VT

In addition to increased propensity to local β-AR-induced PVCs, the combination of $BaCl_2$ + Caff often led to sustained monomorphic VT (defined as ≥3 consecutive

ectopic beats with similar ECG morphology; Fig. 3*A*). Importantly, no sustained arrhythmia of any mechanism was ever induced under any other condition (control, $BaCl_2$, or Caff alone), indicating that the combined effects of $BaCl_2$ + Caff are uniquely arrhythmogenic in this model. A representative example of sustained VT with $BaCl_2$ + Caff is shown in Fig. 3. The ECG (Fig. 3*A*) shows three consecutive beats of intrinsic (junctional) rhythm prior to arrhythmia. These beats have a narrow QRS complex and rapid breakthrough of epicardial activation, as can be observed in the activation maps (Fig. 3*B*, intrinsic rhythm). Following NA application, one PVC of

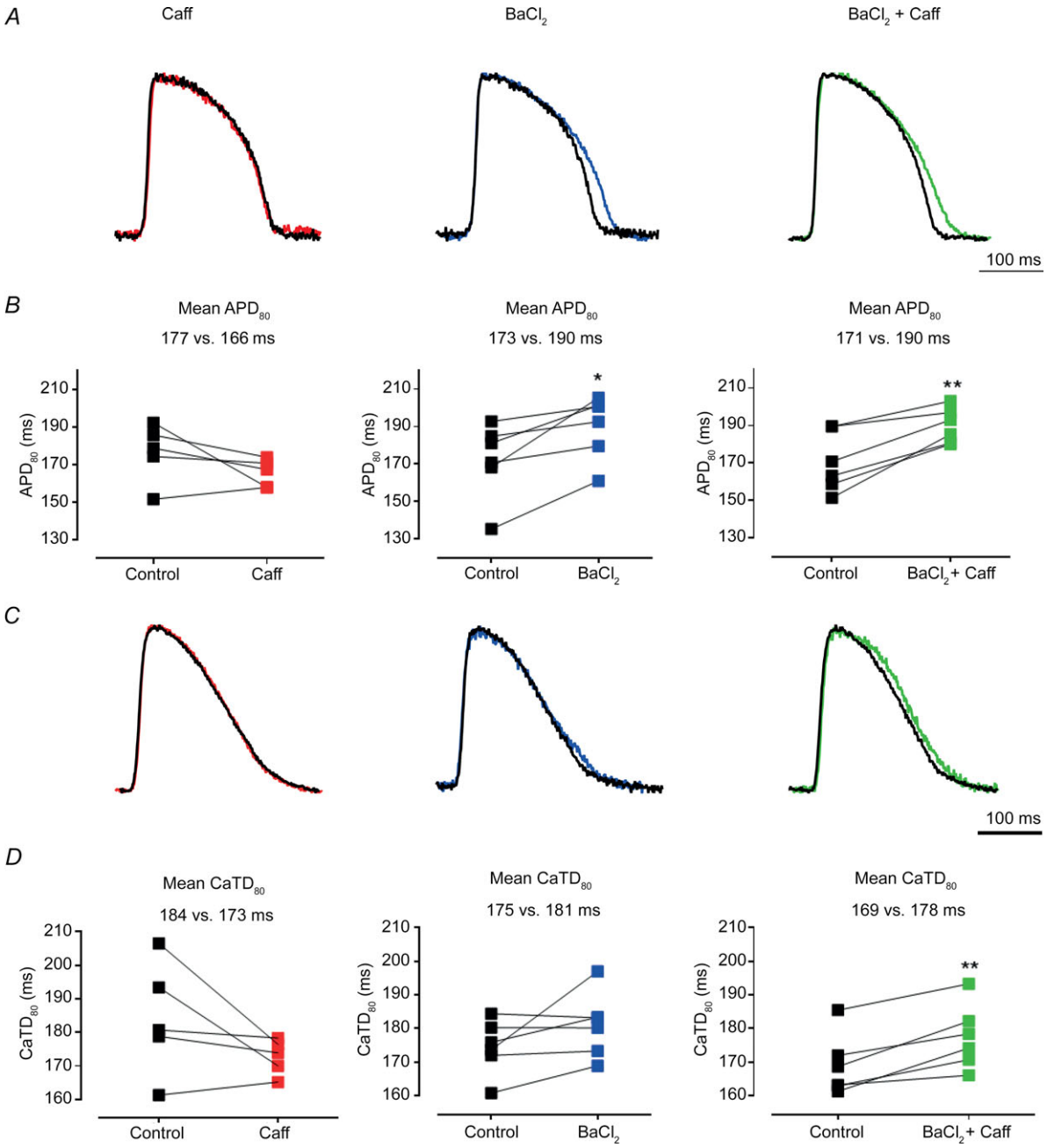

Figure 1. Effects of Caff, $BaCl_2$ and $BaCl_2$ + Caff on action potentials (APs) and Ca^{2+} transients (CaTs)
A, superimposed APs before and after Caff (black and red traces), before and after $BaCl_2$ (black and blue) and before and after the combination of $BaCl_2$ + Caff (black and green). *B*, graphs showing change in APD_{80} with Caff, $BaCl_2$ and $BaCl_2$ + Caff in each heart, with mean values given. *C*, superimposed CaTs before and after Caff (black and red traces), before and after $BaCl_2$ (black and blue), and before and after the combination of $BaCl_2$ + Caff (black and green). *D*, graphs showing change in $CaTD_{80}$ with Caff, $BaCl_2$ and $BaCl_2$ + Caff in each heart, with mean values given. Data were compared using a paired Student's *t* test, $^*P < 0.05$, $^{**}P < 0.01$.

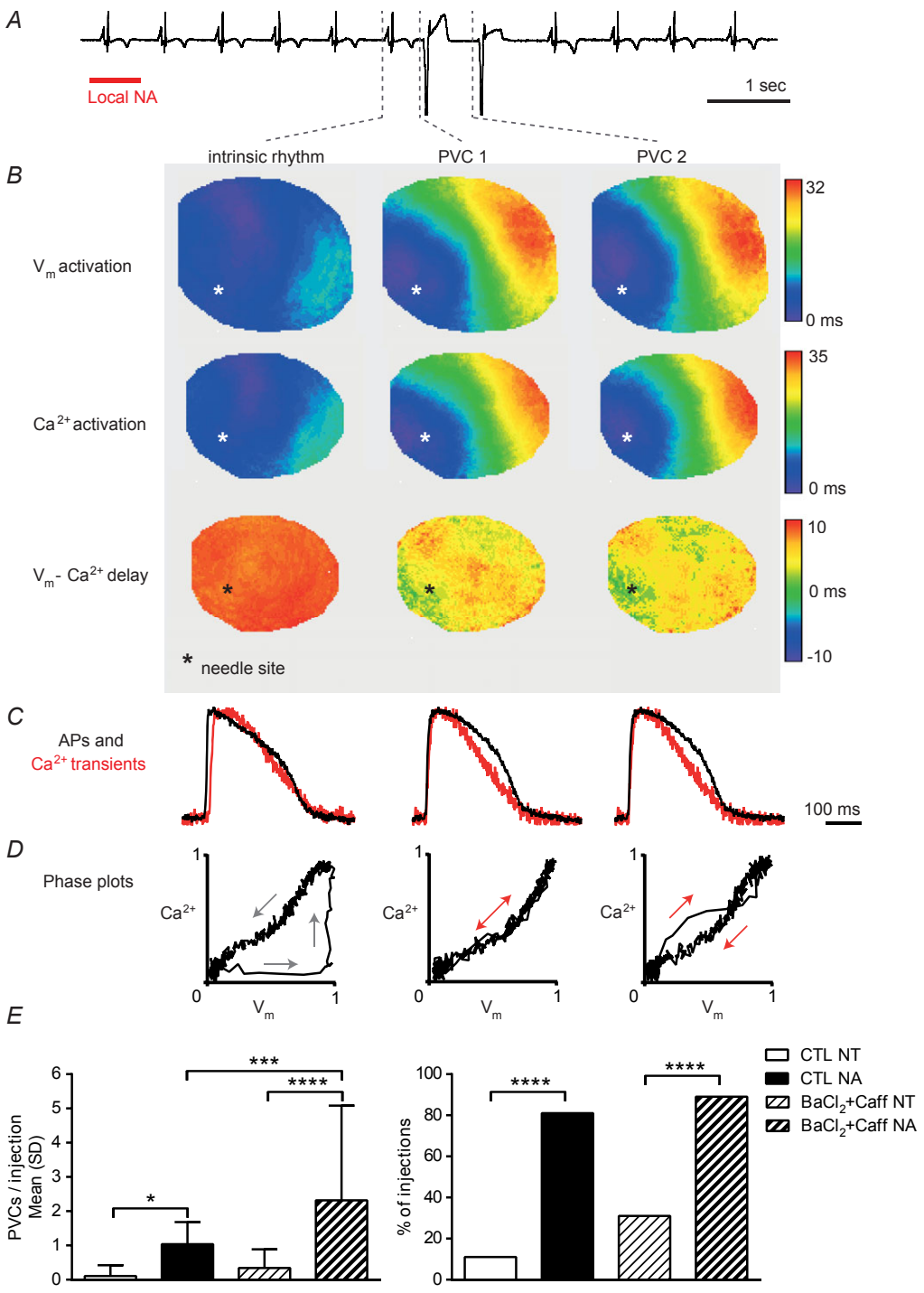

Figure 2. Induction of premature ventricular complexes (PVCs) with local noradrenaline (NA) application
A, ECG during local NA application showing the induction of two PVCs. *B*, V_m activation maps for the last beat of intrinsic rhythm, the first and second PVCs (PVC 1, PVC 2), showing earliest epicardial activation during intrinsic rhythm distant from the needle site (*) and activation arising from the needle site during PVCs. Ca^{2+} activation maps are also shown, along with V_m–Ca^{2+} delay maps for each, indicating abnormal V_m–Ca^{2+} delay (~0–2 ms, green areas) around the NA application site during PVCs. *C*, superimposed APs (black traces) and Ca^{2+} transients (red traces), from the site of earliest epicardial activation. *D*, corresponding V_m/Ca^{2+} phase plots demonstrate the abnormal V_m/Ca^{2+} relationship at sites of focal activation during PVCs. *E*, summary data for the occurrence of PVCs following local application of normal Tyrode solution (NT, open bars) and NA (filled bars), under control conditions and in the presence of $BaCl_2$ + Caff (hatched bars). Continuous data were compared using a one-way ANOVA with Bonferroni post testing and categorical testing using Fisher's exact test. *$P < 0.05$, ***$P < 0.001$, ****$P < 0.0001$.

Table 1. PVC occurrence

	CTL ($n = 15$)	$BaCl_2$ ($n = 6$)	Caff ($n = 5$)	$BaCl_2$ + Caff ($n = 6$)	P
PVCs/NT injection, mean (SD)	0.2 (0.5)	0.3 (0.6)	0.6 (0.8)	0.3 (0.5)	NS
PVCs/NA injection, mean (SD)	1.1 (0.7)	1.0 (0.7)	1.3 (0.8)	2.3 (2.8)*	*<0.05 *vs.* CTL, $BaCl_2$, Caff
P	<0.05	<0.05	<0.05	<0.001	

$BaCl_2$, barium chloride; Caff, caffeine; CTL, control; NA, noradrenaline, NS, non-significant; NT, normal Tyrode solution; PVC, premature ventricular complex; SD, standard deviation. Data were compared using a two-way ANOVA with Bonferroni post tests.

distinct morphology can be observed on both the ECG and activation map (Fig. 3*B*, PVC). The earliest excitation of this PVC arises from very near the needle location (marked with an asterisk) and excitation propagates more slowly than during intrinsic rhythm. Interestingly, immediately following this PVC, sustained focal VT develops. Both the ECG morphology and activation sequence of the VT are slightly different from those of the PVC, but activation still arises from very near the needle location (albeit not exactly the same location as the PVC, Fig. 3*B*, VT 1 and VT 2). Only two beats of the VT were optically recorded in this example; however, the VT persisted for 7 s. The V_m –Ca^{2+} delay maps again suggested pathological early Ca^{2+} release at the site of initiation of the PVC and this abnormal V_m –Ca^{2+} delay was also evident during the focal VT. This can also be seen in the superimposed upstrokes and the V_m/Ca^{2+} phase plots, which strongly suggest a Ca^{2+}-driven mechanism for this focal VT (Fig. 3*C* and *D*).

In total, 15 episodes of sustained monomorphic VT occurred directly following NA injections (as in Fig. 3) in 4/6 hearts in which $BaCl_2$ + Caff was applied (Table 2). To distinguish this type of arrhythmia from VT that occurred later following NA injection, we have termed this 'early VT'. Early VT had a mean cycle length of 657 ms and a mean duration of 7 s. Thirteen out of 15 (87%) early VT episodes were initiated following one or more PVCs of a distinct morphology before transition to stable focal VT (as in Fig. 3). The remaining two early VT episodes, however, maintained the same morphology from the very first beat (i.e. no distinct PVCs prior to VT).

Late VT

Interestingly, even more frequent than early VT was VT occurring later ('late VT', 17.4 ± 9.2 *vs.* 4.8 ± 0.5 s, $P < 0.0001$) following NA injection. Late VT occurred either following early VT and a brief return to instrinic rhythm (as in Fig. 4*A*) or even in the absence of early VT (as in Fig. 4*B*). Figure 4*A* shows the typical progression of early and late VT following local β-AR stimulation. After two beats of intrinsic (sinus) rhythm, a single PVC occurs, followed immediately by sustained focal early VT, in which the ECG shows a different morphology from that of the PVC. Early VT continues for 18 beats (11 s) before spontaneously returning to sinus rhythm. Then, following three sinus beats, late VT initiates, with the same ECG morphology as early VT. In this example, late VT continued for 74 s before the rate slowed and VT spontaneously terminated. Figure 4*A* also illustrates an attempt to terminate late VT with ventricular overdrive pacing (VOP). As can be observed, VOP is applied at a higher frequency than the late VT and pacing is able to capture the ventricles for the duration of VOP. However, immediately upon cessation of pacing, late VT resumes with similar rate and morphology. There is no evidence of QRS fusion during VOP, and the ventricles are not entrained to the pacing cycle length on cessation of VOP, both of which features argue against a re-entrant mechanism and strongly suggest a focal VT mechanism (Arnar *et al.* 2005).

In total, 32 episodes of monomorphic late VT occurred following a total of 64 local NA applications in 6/6 hearts in the presence of $BaCl_2$ + Caff (Table 1). Late VT was significantly more common than early VT following NA application in the presence of $BaCl_2$ + Caff (50 *vs.* 23%, $P < 0.001$). Late VT had a significantly shorter cycle length compared to early VT (359 *vs.* 657 ms, respectively, $P < 0.0001$) and a longer duration (166 *vs.* 7 s, $P < 0.0001$). In contrast to early VT, late VT was not initiated by PVCs of distinct morphology, but rather had the same ECG morphology from the onset (Fig. 4*A and B*). Late VT typically accelerated after initiation and then progressively slowed prior to termination. VOP captured the ventricles but did not entrain or terminate late VT, suggesting a focal arrhythmia mechanism.

Mechanisms of focal arrhythmia with $BaCl_2$ + Caff

Figure 5 shows the ECG, activation and V_m–Ca^{2+} delay maps, and representative traces during a typical example of late VT. Activation maps are shown for three consecutive beats of late VT; however, activation remained stable throughout late VT with the site of earliest activation

emerging from the site of local NA application (Fig. 5*B*, white square). Example V_m and Ca^{2+} traces from a site of early, mid and late activation during late VT are shown in Fig. 5*C*. Although the traces from the mid (grey square) and late (black square) sites show normal excitation–contraction coupling (Ca^{2+} rising after membrane depolarization, Fig. 5*D* and *E*) and APD and CaTD of similar durations (Fig. 5*C* and *D*), the traces from the site of earliest activation show deranged excitation–contraction coupling and abbreviated CaTD relative to the APD at this site. Consistent with local β-AR stimulation at the site of NA application, the time

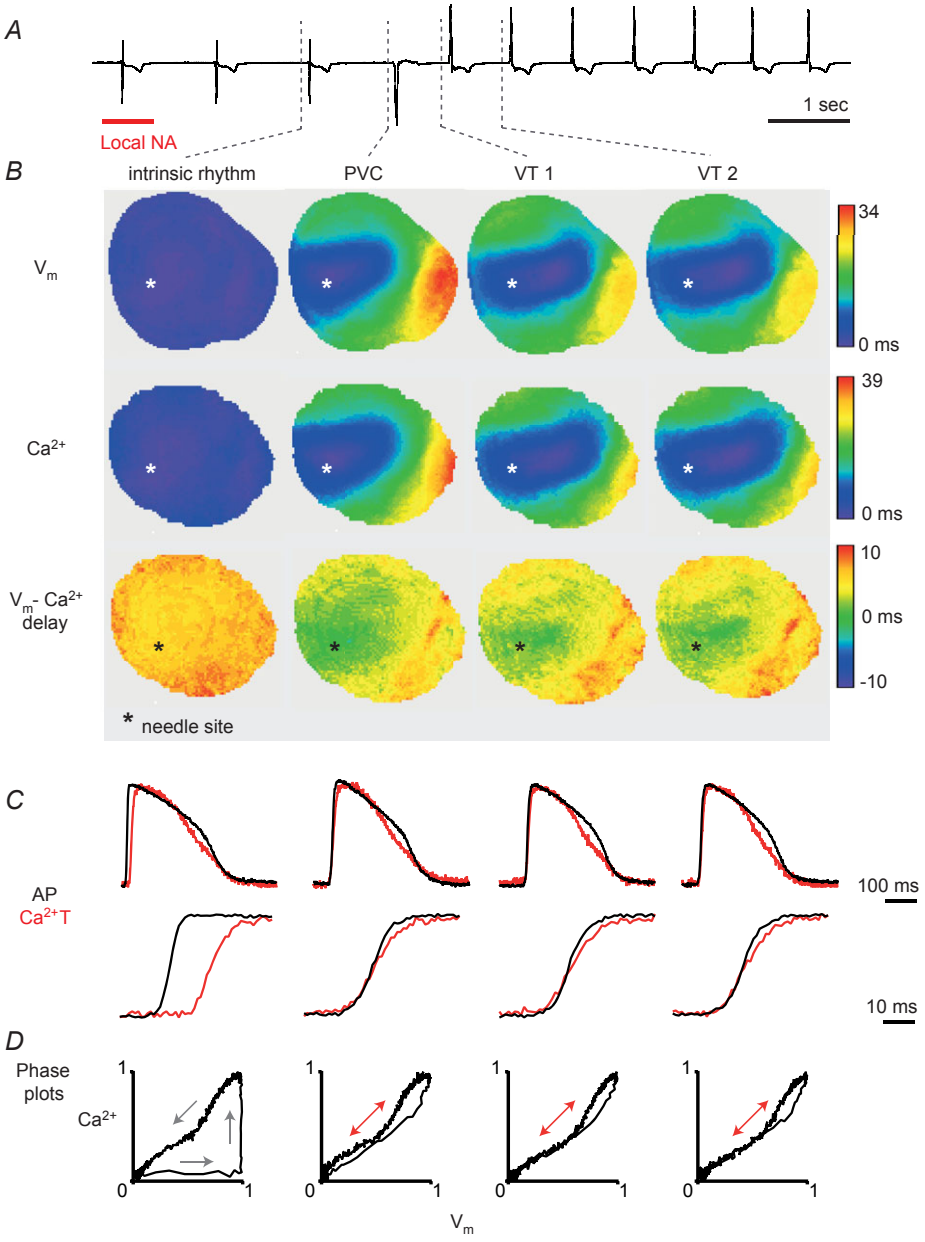

Figure 3. Induction of early ventricular tachycardia (VT) with local NA application in the presence of $BaCl_2$ + Caff
A, ECG during the induction of early VT following an NA-induced PVC in the presence of $BaCl_2$ + Caff. *B*, V_m maps for the last beat of intrinsic rhythm, the PVC and the first two beats of early VT (VT 1 and VT 2). Both the PVC and VT show earliest epicardial activation near the needle site (*). Ca^{2+} activation maps are also shown, along with V_m–Ca^{2+} delay maps for each beat, indicating the abnormal V_m–Ca^{2+} delay (~0–2 ms, green area) around the NA application site during PVCs and early VT. *C*, superimposed APs (black) and Ca^{2+} transients (red), sampled from the site of earliest epicardial activation with expanded traces to show the upstrokes. *D*, corresponding V_m/Ca^{2+} phase plots demonstrate the abnormal V_m/Ca^{2+} relationship at sites of focal activation during PVCs and early VT.

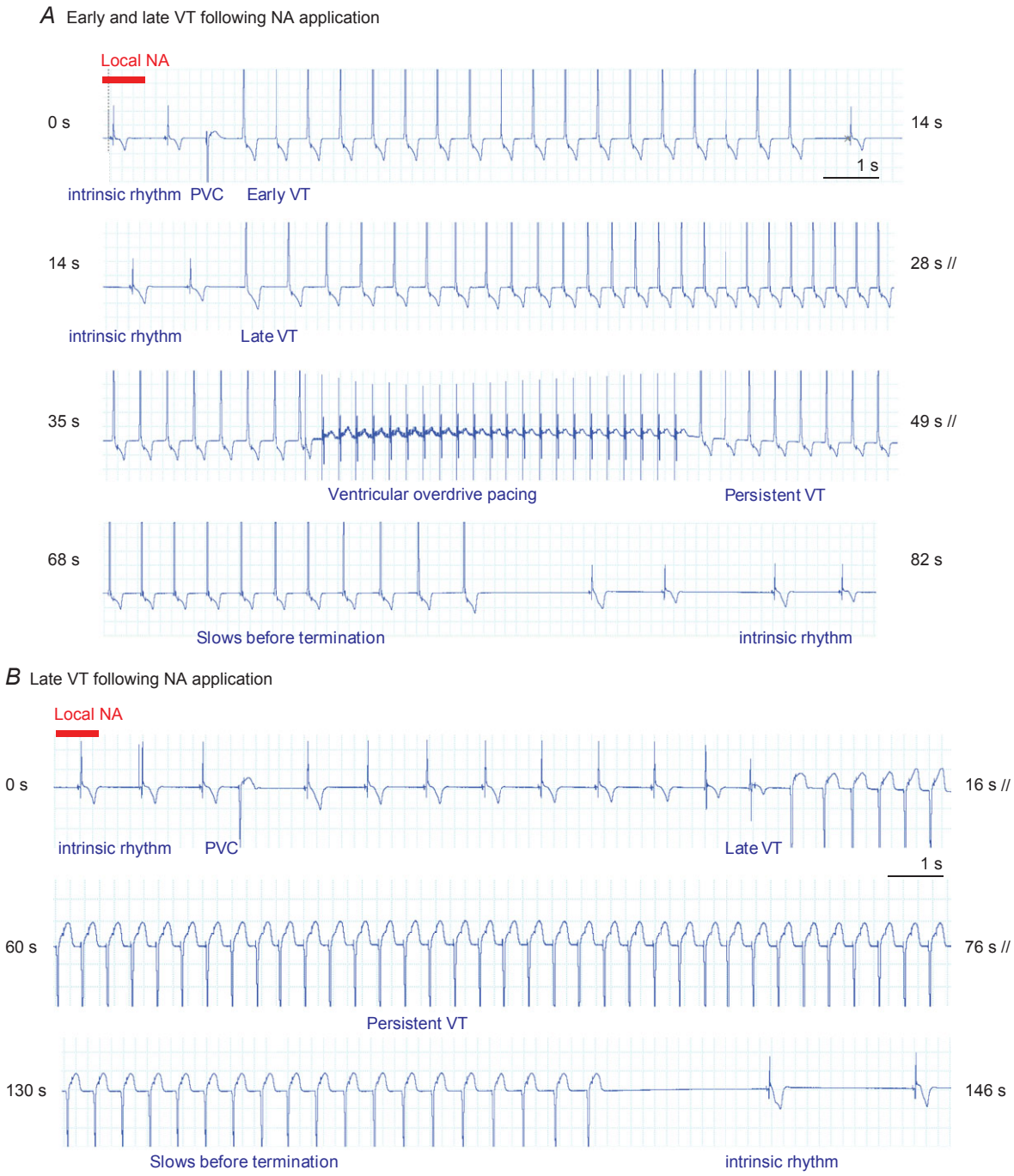

Figure 4. ECG recordings during initiation, maintenance and termination of early and late ventricular tachycardia (VT)
A, ECG recording of early and late VT induced by local noradrenaline (NA) in the presence of $BaCl_2$ + Caff. Local NA is administered during intrinsic (sinus) rhythm and induces a premature ventricular complex (PVC), which is immediately followed by early VT. The broad QRS and retrograde atrial activation are evident in both the PVC and VT. Early VT is monomorphic and persists for 11 s at a stable cycle length (CL) of 570 ms before terminating and sinus rhythm resumes for 3 beats. Late VT then initiates, with a similar ECG morphology and a progressive increase in rate to a CL of 365 ms. Ventricular overdrive pacing at a CL of 300 ms is then applied but does not terminate late VT. Late VT then slows and terminates spontaneously after a total of 74 s. *B*, ECG recording of late VT induced by local NA application in the presence of $BaCl_2$ + Caff taken from the same heart as *A* but with NA application at a different site. Local NA is administered during intrinsic (sinus) rhythm and induces a PVC, which is immediately followed by resumption of sinus rhythm. Late monomorphic VT then starts, with a similar ECG morphology to the PVC and progressively increases in rate to a CL of 320 ms. Late VT then slows and spontaneously terminates after a total duration of 135 s. // indicates a break in continuity between the ECG tracings.

constant of Ca^{2+} decay (τ) is considerably faster at this site (Fig. 5*D*), suggesting β-AR-mediated acceleration of sarcoplasmic reticulum Ca^{2+} ATPase (SERCA) activity. The expanded traces (Fig. 5*D*) also show diastolic Ca^{2+} elevation, slight diastolic membrane depolarization, and the V_m and Ca^{2+} upstrokes occurring nearly simultaneously, indicating pathological early Ca^{2+} release. Collectively, these data suggest that the combination of $BaCl_2$ + Caff is particularly arrhythmogenic during local β-AR stimulation because the β-AR-mediated local

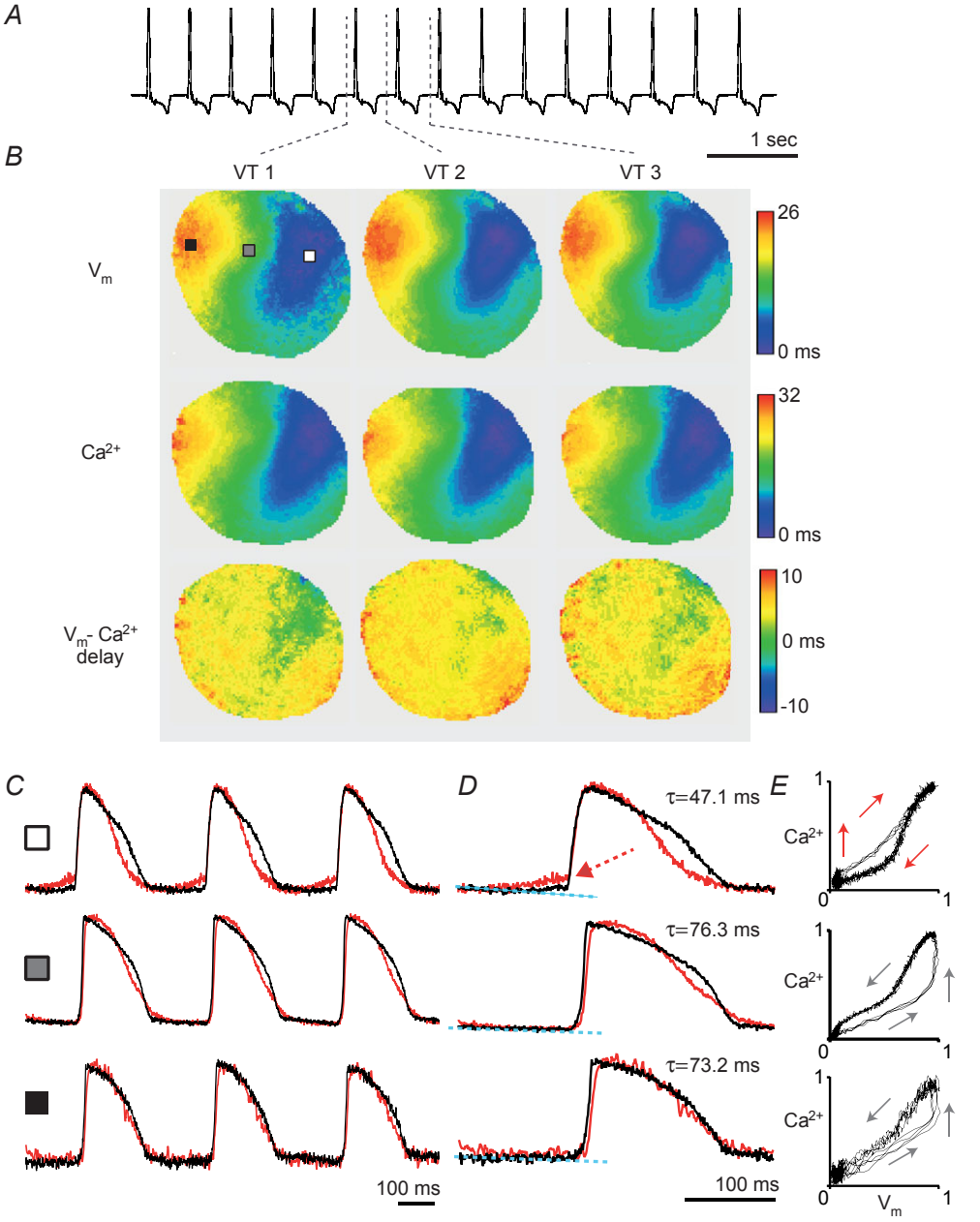

Figure 5. Late VT following local NA application in the presence of $BaCl_2$ + Caff
A, ECG recording of late VT 16 s after NA application in the presence of $BaCl_2$ + Caff. *B*, V_m maps for 3 beats of late VT (VT 1, VT 2 and VT 3) showing earliest epicardial activation from close to the needle site. Ca^{2+} activation maps are also shown, along with V_m–Ca^{2+} delay maps for each beat, indicating the abnormal V_m–Ca^{2+} delay (~0–2 ms, green area) around the NA application site during late VT. *C*, superimposed APs (black traces) and Ca^{2+} transients (red traces), from the sites shown by the squares in *B*, corresponding to an early activated epicardial site (white square), a site activated at the midpoint of the epicardial spread of depolarization (grey square) and a late-activated site (black square). Expanded traces (*D*) and corresponding phase plots (*E*) are also shown. At the site of earliest epicardial activation there is clear diastolic Ca^{2+} elevation, which precedes V_m activation and is not seen at later activated sites. The time constant of Ca^{2+} decay (τ) is also abbreviated at the earliest activated site.

Table 2. VT occurrence and characteristics

	Early VT ($n = 15$)	Late VT ($n = 32$)	P
Hearts with VT following local NA, *n* (%)	4 (67)	6 (100)	NS
%NA injections resulting in VT	23	50	<0.01
Time after injection (s), mean (SD)	4.8 (0.5)	17.4 (9.2)	<0.0001
Initiated by PVC(s), *n* (%)	13 (87)	0 (0)	<0.0001
Monomorphic, *n* (%)	15 (100)	28 (100)	NS
QRS duration (ms), mean (SD)	58 (10)	59 (8)	NS
Cycle length (ms), mean (SD)	657 (180)	359 (72)	<0.0001
Duration (s), mean (range)	7 (2–18)	166 (15–397)	<0.0001

ms, milliseconds; NA, noradrenaline, NS, non-significant; PVC, premature ventricular complex; s, seconds; SD, standard deviation; VT, ventricular tachycardia. Data were compared using unpaired *t* tests for continuous data and Fisher's exact test for categorical data.

increase in SERCA activity leads to increased SR Ca^{2+} load and increased spontaneous SR Ca^{2+} release (due to elevated SR Ca^{2+} load and sensitized RyRs with Caff), and that this spontaneous SR Ca^{2+} release can more easily lead to diastolic membrane depolarization due to reduced I_{K1} with $BaCl_2$.

Discussion

The aim of the present study was to determine the role of two key aspects of the complex HF phenotype in contributing to focal arrhythmia during local β-AR stimulation in intact non-failing rabbit hearts. Specifically, we investigated the effects of decreased I_{K1} (with 50 μM $BaCl_2$) and increased RyR sensitivity (with 200 μM Caff), both alone and in combination, and importantly, at magnitudes similar to those seen in HF. We found that (1) local β-AR stimulation with NA produces ventricular ectopic beats (PVCs) arising from the site of stimulation, and these PVCs are likely due to pathological SR Ca^{2+} release, as indicated by the abbreviated V_m–Ca^{2+} delay at the site of earliest activation and reversed chirality of the V_m/Ca^{2+} phase plots (Myles *et al.* 2012); (2) at the pathophysiologically relevant doses studied, neither $BaCl_2$ nor Caff alone led to a significant increase in arrhythmia inducibility during local β-AR stimulation; (3) the combination of $BaCl_2$ + Caff was extremely arrhythmogenic during local β-AR stimulation, resulting in a significant increase in PVCs as well as early and late sustained monomorphic focal VT, which occurred in all hearts. Sustained VT was never observed in response to local β-AR stimulation under any other condition studied (control, $BaCl_2$, Caff) or in previous studies with partial gap junction uncoupling (Myles *et al.* 2012), illustrating the uniquely arrhythmogenic consequences and synergistic combination of decreased I_{K1} and increased RyR sensitivity in contributing to sustained focal arrhythmia in the intact heart.

Focal arrhythmia mechanisms in HF

Although re-entry may be responsible for initiation and maintenance of VT in many pathological states, there is compelling evidence that VT in non-ischaemic HF can be driven by focal (non-re-entrant) mechanisms. Spontaneous and inducible focal VT have been observed in 3-dimensional mapping studies from failing human (Pogwizd *et al.* 1998) and rabbit hearts (Pogwizd, 1995) and similar activity has been optically recorded in the failing canine heart (Hoeker *et al.* 2009). At the cellular level, many components of HF remodelling may conspire to increase the likelihood of spontaneous Ca^{2+} release from the SR, including increased RyR sensitivity (Shannon *et al.* 2003) and preserved β-AR responsiveness (Pogwizd *et al.* 2001). Furthermore, HF myocytes have enhanced NCX function (Pogwizd *et al.* 1999), decreased gap junction coupling (Dupont *et al.* 2001), and decreased inward rectifying K^+ current (I_{K1}) (Pogwizd *et al.* 2001). Therefore, when spontaneous Ca^{2+} release occurs, it generates a larger transient inward current (I_{ti}, carried by NCX), which can then more easily depolarize the resting membrane (due to decreased I_{K1}) to produce a triggered action potential (Puglisi & Bers, 2001).

Previously, we showed that partial gap junction uncoupling leads to a significantly increased propensity to PVCs in response to local β-AR stimulation (Myles *et al.* 2012); however, no sustained arrhythmias were observed. Therefore, in the present study, we sought to determine the impact of additional aspects of the HF phenotype, both alone and in combination, on the propensity to PVCs and focal activity during local β-AR stimulation in non-failing hearts. In this regard, we selected two key phenotypes that were relatively easy to manipulate pharmacologically and likely to have an impact on the generation and escape of focal activity.

Increased RyR sensitivity (via increased RyR open probability) decreases the threshold for spontaneous SR Ca^{2+} release (Venetucci *et al.* 2008). This means that when RyR sensitivity is increased, less β-AR stimulation is

required to produce SR Ca^{2+} overload and spontaneous Ca^{2+} release. In addition to contributing to arrhythmia in HF, this is a key mechanism thought to be responsible for focal arrhythmias in catecholaminergic polymorphic ventricular tachycardia (CPVT) (Priori *et al.* 2001; Cerrone *et al.* 2007). We (Wang *et al.* 2014) and others (Trafford *et al.* 1998; Domeier *et al.* 2009) have shown that low-dose caffeine can sensitize RyRs without leading to complete SR Ca^{2+} depletion, as is the case with high-dose caffeine (Trafford *et al.* 1998). Decreased I_{K1}, on the other hand, does not directly impact SR Ca^{2+} handling, but rather destabilizes the resting V_m so that the depolarizing current carried by NCX in response to SR Ca^{2+} release leads to greater membrane depolarization and increases the likelihood of reaching the threshold for an action potential. This is known as increased Ca^{2+}/V_m coupling gain (Maruyama *et al.* 2010). Previous studies have demonstrated a significant increase in focal activity and ventricular escape beats when I_{K1} is reduced with $BaCl_2$ (Foster *et al.* 1977), and have suggested that the reduced repolarization reserve caused by $BaCl_2$ unmasks the pro-arrhythmic potential of other underlying conditions (Wu *et al.* 2009). Correspondingly, potentiation of repolarizing K^+ currents by acute elevation of $[K^+]$ has been shown to reduce the occurrence of sympathetically driven ventricular arrhythmias (O'Neill & Paterson, 1995).

Here we show, for the first time, that the combination of increased RyR sensitivity and decreased I_{K1} produces a strikingly arrhythmogenic phenotype in the intact heart. The frequent occurrence of sustained focal arrhythmia under this condition suggests more than a simple additive effect of either condition alone and indicates a unique synergism between these two pathophysiological phenotypes. This important finding is one that cannot be tested in isolated cells or inferred from single cell studies due to the complex source–sink interactions in the intact heart (Xie *et al.* 2010).

Mechanisms of arrhythmia during localized β-AR stimulation

We (Myles *et al.* 2012) and others (Podzuweit, 1980; Nash *et al.* 2001; Doppalapudi *et al.* 2008) have previously reported on the mechanisms of ventricular tachyarrhythmias during localized β-AR stimulation. Indeed, local release of catecholamines can occur in a number of pathologies including acute, regional ischaemia (Schömig *et al.* 1987) and following chronic remodelling of the intrinsic cardiac innervation (Li *et al.* 2004), making local β-AR stimulation a pathophysiologically relevant arrhythmia paradigm. Most previous studies, however, have employed sustained infusion of a relatively low concentration of NA (10 μM, 150 μl min^{-1} in Nash *et al.* for example). In normal porcine hearts, this continuous NA infusion results in sustained focal VT arising from the infusion site that lasts for the duration of infusion. Here, we employed a slightly different approach with a single bolus infusion of a small volume (50 μl) of 250 μM NA. Intrasynaptic NA concentrations in vascular nerve terminals have been measured at up to 100 μM, with an inverse relationship between intrasynaptic NA concentration and the size of the junctional space reported (Bevan & Su, 1974). Because the cardiac neuroeffector junctions are narrower than vascular junctions, the concentration used in our study may be similar to NA concentrations during physiological nerve stimulation, especially in HF, when sympathetic drive is high (Hasking *et al.* 1986).

Under control, $BaCl_2$ alone, and Caff alone conditions, a single dose of NA results in only 1–3 isolated PVCs arising from the application site (Fig. 2). Presumably, as the NA diffuses away from the injection site, the concentration is no longer high enough locally to elicit additional PVCs or arrhythmogenic activity. However, when hearts are pre-treated with $BaCl_2$ + Caff, sustained focal VT develops arising from the injection site and lasting up to 397 s (~6 min) after the single bolus injection. Interestingly, both early and late VT often originated from a site slightly different from that of the initial PVCs (Figs 3 and 5), but still very near the NA injection site. This site of focal activity was reproducible, with VT emerging from this same location after repeated infusions from the same needle location. This may suggest that the initial high local concentration of NA elicits PVCs directly at the site of stimulation; however, as the NA diffuses locally, a new site of ventricular automaticity emerges, which sustains the VT for the duration of arrhythmia. This local automatic site may represent an area of tissue with increased β-AR responsiveness, increased SERCA activity, increased Ca^{2+}–V_m coupling gain, or perhaps has the shortest RyR refractory period. This last possibility is especially intriguing as it suggests that dominant focal VT sources could emerge in much the same way as dominant pacemakers in the conduction system, with the pacemaker with the shortest cycle length in any given situation taking over as the dominant pacemaker in the system. These mechanisms of dominant VT sources remain an area of future investigation.

Both early and late VT were initiated via changes in intracellular Ca^{2+} rather than through normal excitation–contraction coupling. Some injection sites showed both early and late VT and in some cases, the intrinsic rhythm overdrove the early VT before the late VT emerged, suggesting a similar mechanism for the two arrhythmias. Late VT, however, was characterized by clear diastolic Ca^{2+}elevation (Fig. 5*C* and *D*), suggesting significant SR Ca^{2+} overload. We propose that in PVCs and early VT, very localized β-AR stimulation leads

to spontaneous SR Ca^{2+} release and focal arrhythmia, whereas in late VT a larger area of β-AR stimulation develops resulting in more sustained Ca^{2+} overload, exemplified by the faster rates. This is consistent with the findings of computational modelling in previous studies of local NA-induced ventricular arrhythmia, in which local Ca^{2+} overload triggering focal activity was implicated as the mechanism (Nash *et al.* 2001). In that study, an area of NA-affected cells was modelled within a 2-dimensional sheet. This area displayed spontaneous depolarization which was of sufficient magnitude to generate a propagating wave of depolarization within the cell network. The ionic model revealed that β-AR effects on the L-type Ca^{2+} current I_{CaL} and SERCA resulted in SR Ca^{2+} overload and release with consequent Ca^{2+} extrusion from the cell via NCX, producing membrane depolarization and focal arrhythmia.

Role of decreased I_{K1} and increased RyR sensitivity in contributing to focal arrhythmia

The results of this study suggest that at the pathophysiologically relevant doses tested, neither decreased I_{K1} nor increased RyR sensitivity alone are particularly arrhythmogenic. However, when combined, sustained focal VT developed in response to local β-AR stimulation in every heart studied. This sustained VT was never observed under any other condition and appears to be more severe than a simple additive effect of the two conditions, suggesting synergism between these two key HF phenotypic characteristics. In these experiments, when RyR alone was sensitized, local β-AR stimulation probably resulted in a decreased threshold for spontaneous SR Ca^{2+} release (Venetucci *et al.* 2008). However, because I_{K1} was unaltered and the resting membrane potential was relatively stable, this Ca^{2+} release did not result in a significant increase in PVCs compared to control conditions. Likewise, when I_{K1} alone was reduced, but SR Ca^{2+} release was unaltered, no significant increase in PVC propensity was observed. When combined, however, the reduced threshold for SR Ca^{2+} release (RyR sensitization) and destabilized resting V_m (reduced I_{K1}) resulted in a marked increase in focal activity.

The combination of these mechanisms can be observed in the V_m and Ca^{2+} traces during late VT with $BaCl_2$ + Caff (Fig. 5*C* and *D*). During diastole, significant SR Ca^{2+} leak is observed, manifested as diastolic $[Ca^{2+}]_i$ elevation (arrow in Fig. 5*D*). This increase in $[Ca^{2+}]_i$ leads to a depolarizing inward current (carried by NCX) that, due to the decreased I_{K1}, leads to slight diastolic membrane depolarization (arrow in Fig. 5*D*). This diastolic V_m and Ca^{2+} elevation is not observed at sites far from the VT initiation site (Fig. 5*D*, mid and late sites), nor is it observed during PVCs under control, $BaCl_2$, or Caff alone conditions, in which a single Ca^{2+} release event triggers a single PVC, but focal activity is not sustained.

Limitations

The rates of VT observed in the present study may not be considered tachycardic for a rabbit *in vivo*, but are faster than the typical *ex vivo* heart rates during Langendorff perfusion (Fedorov *et al.* 2007). It is also noteworthy that previous studies of local NA-induced focal VT have shown similarly modest rates but with profound associated haemodynamic compromise as a result of the altered activation sequence (Nash *et al.* 2001). In addition to sensitizing RyRs, Caff is also a weak phosphodiesterase (PDE) inhibitor and may therefore have additional effects on intracellular Ca^{2+} handling, perhaps via increased SERCA activity. However, in the present study, no significant impact on CaTD was observed following Caff application, nor was the time constant of recovery of the SR Ca^{2+} transient found to be affected in a previous study (Wang *et al.* 2014), suggesting the PDE inhibition effect of Caff may be minimal at this dose. While these results may have important implications for our understanding of focal arrhythmia mechanisms in HF, there are many other changes that occur in HF which probably influence the generation of focal arrhythmia. These include fibrosis, gap junction remodelling, changes in ionic currents including NCX, modulation of SERCA, remodelling of the sympathetic nerves, and changes in β-AR signalling (Tomaselli & Zipes, 2004). These and other pathological phenotypes in HF remain an area of future investigation.

Conclusions

Here, we demonstrate for the first time, that marked synergism exists between reduced I_{K1} and increased RyR sensitivity, which leads to a significantly increased propensity to sustained focal arrhythmia in the intact non-failing rabbit heart. In isolation, neither of these key HF phenotypic characteristics were arrhythmogenic in this model. However, in combination they led to frequent and sustained ventricular arrhythmias. This finding, to our knowledge, has not been previously reported in the intact heart and may have important clinical implications for the understanding and prevention of focal arrhythmia in HF and may suggest novel therapeutic strategies.

References

Arnar DO, Xing D & Martins JB (2005). Overdrive pacing of early ischemic ventricular tachycardia: evidence for both reentry and triggered activity. *Am J Physiol Heart Circ Physiol* **288**, H1124–H1130.

Baker DW, Einstadter D, Thomas C & Cebul RD (2003). Mortality trends for 23505 Medicare patients hospitalized with heart failure in Northeast Ohio, 1991 to 1997. *Am Heart J* **146**, 258–264.

Bevan JA & Su C (1974). Variation of intra- and perisynaptic adrenergic transmitter concentrations with width of synaptic cleft in vascular tissue. *J Pharmacol Exp Ther* **190**, 30–38.

Cerrone M, Noujaim SF, Tolkacheva EG, Talkachou A, O'Connell R, Berenfeld O, Anumonwo J, Pandit SV, Vikstrom K, Napolitano C, Priori SG & Jalife J (2007). Arrhythmogenic mechanisms in a mouse model of catecholaminergic polymorphic ventricular tachycardia. *Circ Res* **101**, 1039–1048.

Choi B-R, Burton F & Salama G (2002). Cytosolic Ca^{2+} triggers early afterdepolarizations and torsade de pointes in rabbit hearts with type 2 long QT syndrome. *J Physiol* **543**, 615–631.

Domeier TL, Blatter LA & Zima AV (2009). Alteration of sarcoplasmic reticulum Ca^{2+} release termination by ryanodine receptor sensitization and in heart failure. *J Physiol* **587**, 5197–5209.

Doppalapudi H, Jin Q, Dosdall DJ, Qin H, Walcott GP, Killingsworth CR, Smith WM, Ideker RE & Huang J (2008). Intracoronary infusion of catecholamines causes focal arrhythmias in pigs. *J Cardiovasc Electrophysiol* **19**, 963–970.

Drummond GB (2009). Reporting ethical matters in *The Journal of Physiology*: standards and advice. *J Physiol* **587**, 713–719.

Dupont E, Matsushita T, Kaba RA, Vozzi C, Coppen SR, Khan N, Kaprielian R, Yacoub MH & Severs NJ (2001). Altered connexin expression in human congestive heart failure. *J Mol Cell Cardiol* **33**, 359–371.

Fedorov VV, Lozinsky IT, Sosunov EA, Anyukhovsky EP, Rosen MR, Balke CW & Efimov IR (2007). Application of blebbistatin as an excitation-contraction uncoupler for electrophysiologic study of rat and rabbit hearts. *Heart Rhythm* **4**, 619–626.

Foster PR, Elharrar V & Zipes DP (1977). Accelerated ventricular escapes induced in the intact dog by barium, strontium and calcium. *J Pharmacol Exp Ther* **200**, 373–383.

Hasking GJ, Esler MD, Jennings GL, Burton D, Johns JA & Korner PI (1986). Norepinephrine spillover to plasma in patients with congestive heart failure: evidence of increased overall and cardiorenal sympathetic nervous activity. *Circulation* **73**, 615–621.

Hoeker GS, Katra RP, Wilson LD, Plummer BN & Laurita KR (2009). Spontaneous calcium release in tissue from the failing canine heart. *Am J Physiol Heart Circ Physiol* **297**, H1235–H1242.

Huikuri HV, Castellanos A & Myerburg RJ (2001). Sudden death due to cardiac arrhythmias. *N Engl J Med* **345**, 1473–1482.

Joyner RW & van Capelle FJ (1986). Propagation through electrically coupled cells. How a small SA node drives a large atrium. *Biophys J* **50**, 1157–1164.

Laurita KR, Katra R, Wible B, Wan X & Koo MH (2003). Transmural heterogeneity of calcium handling in canine. *Circ Res* **92**, 668–675.

Li W, Knowlton D, Van Winkle DM & Habecker BA (2004). Infarction alters both the distribution and noradrenergic properties of cardiac sympathetic neurons. *Am J Physiol Heart Circ Physiol* **286**, H2229–H2236.

McMurray JJV & Pfeffer MA (2005). Heart failure. *Lancet* **365**, 1877–1889.

Maruyama M, Joung B, Tang L, Shinohara T, On Y-K, Han S, Choi E-K, Kim D-H, Shen MJ, Weiss JN, Lin S-F & Chen P-S (2010). Diastolic intracellular calcium-membrane voltage coupling gain and postshock arrhythmias: role of Purkinje fibers and triggered activity. *Circ Res* **106**, 399–408.

Myles RC, Wang L, Kang C, Bers DM & Ripplinger CM (2012). Local β-adrenergic stimulation overcomes source-sink mismatch to generate focal arrhythmia. *Circ Res* **110**, 1454–1464.

Nash MP, Thornton JM, Sears CE, Varghese A, O'Neill M & Paterson DJ (2001). Ventricular activation during sympathetic imbalance and its computational reconstruction. *J Appl Physiol* **90**, 287–298.

O'Neill M & Paterson DJ (1995). Role of the sympathetic nervous system in cardiac performance during hyperkalaemia in the anaesthetized pig. *Acta Physiol Scand* **153**, 1–11.

Podzuweit T (1980). Catecholamine-cyclic-AMP-Ca^{2+}-induced ventricular tachycardia in the intact pig heart. *Basic Res Cardiol* **75**, 772–779.

Pogwizd SM (1995). Nonreentrant mechanisms underlying spontaneous ventricular arrhythmias in a model of nonischemic heart failure in rabbits. *Circulation* **92**, 1034–1048.

Pogwizd SM, McKenzie JP & Cain ME (1998). Mechanisms underlying spontaneous and induced ventricular arrhythmias in patients with idiopathic dilated cardiomyopathy. *Circulation* **98**, 2404–2414.

Pogwizd SM, Qi M, Yuan W, Samarel AM & Bers DM (1999). Upregulation of Na^+/Ca^{2+} exchanger expression and function in an arrhythmogenic rabbit model of heart failure. *Circ Res* **85**, 1009–1019.

Pogwizd SM, Schlotthauer K, Li L, Yuan W & Bers DM (2001). Arrhythmogenesis and contractile dysfunction in heart failure: Roles of sodium-calcium exchange, inward rectifier potassium current, and residual β-adrenergic responsiveness. *Circ Res* **88**, 1159–1167.

Priori SG, Napolitano C, Tiso N, Memmi M, Vignati G, Bloise R, Sorrentino V & Danieli GA (2001). Mutations in the cardiac ryanodine receptor gene (*hRyR2*) underlie catecholaminergic polymorphic ventricular tachycardia. *Circulation* **103**, 196–200.

Puglisi JL & Bers DM (2001). LabHEART: an interactive computer model of rabbit ventricular myocyte ion channels and Ca transport. *Am J Physiol Cell Physiol* **281**, C2049–C2060.

Schömig A, Fischer S, Kurz T, Richardt G & Schömig E (1987). Nonexocytotic release of endogenous noradrenaline in the ischemic and anoxic rat heart: mechanism and metabolic requirements. *Circ Res* **60**, 194–205.

Shannon TR, Pogwizd SM & Bers DM (2003). Elevated sarcoplasmic reticulum Ca^{2+} leak in intact ventricular myocytes from rabbits in heart failure. *Circ Res* **93**, 592–594.
Tomaselli GF & Zipes DP (2004). What causes sudden death in heart failure? *Circ Res* **95**, 754–763.
Trafford AW, Díaz ME & Eisner DA (1998). Stimulation of Ca-induced Ca release only transiently increases the systolic Ca transient: measurements of Ca fluxes and sarcoplasmic reticulum Ca. *Cardiovasc Res* **37**, 710–717.
Venetucci LA, Trafford AW, O'Neill SC & Eisner DA (2008). The sarcoplasmic reticulum and arrhythmogenic calcium release. *Cardiovasc Res* **77**, 285–292.
Vermeulen JT, McGuire MA, Opthof T, Coronel R, de Bakker JM, Klöpping C & Janse MJ (1994). Triggered activity and automaticity in ventricular trabeculae of failing human and rabbit hearts. *Cardiovasc Res* **28**, 1547–1554.
Wang L, Myles RC, De Jesus NM, Ohlendorf AKP, Bers DM & Ripplinger CM (2014). Optical mapping of sarcoplasmic reticulum Ca^{2+} in the intact heart: ryanodine receptor refractoriness during alternans and fibrillation. *Circ Res* **114**, 1410–1421.
Wu L, Rajamani S, Li H, January CT, Shryock JC & Belardinelli L (2009). Reduction of repolarization reserve unmasks the proarrhythmic role of endogenous late Na^{+} current in the heart. *Am J Physiol Heart Circ Physiol* **297**, H1048–H1057.
Xie Y, Sato D, Garfinkel A, Qu Z & Weiss JN (2010). So little source, so much sink: requirements for afterdepolarizations to propagate in tissue. *Biophys J* **99**, 1408–1415.

Additional information

Competing interests

The authors declare that there are no competing interests.

Author contributions

R.C.M. and C.M.R. conceived the study, designed experiments, interpreted data, and wrote the manuscript. R.C.M. and L.W. performed experiments and analysed data. D.M.B. contributed to the conception and design of experiments, interpretation of data, and manuscript preparation. All experiments were carried out at the University of California, Davis. All authors approved the final version of the manuscript.

Funding

This study was supported in part by the British Heart Foundation (FS/10/64/28532 to R.C.M.), the US National Institutes of Health R01 HL111600 (C.M.R.), P30 HL101280 (C.M.R. and D.M.B.) and P01 HL80101 (D.M.B.), and the American Heart Association 12SDG9010015 (C.M.R.).